Biomaterials 33 (2012) 7765–7774

Contents lists available at SciVerse ScienceDirect

Biomaterials

journal homepage: www.elsevier.com/locate/biomaterials

Hyperbranched polydiselenide as a self assembling broad spectrum anticancer agent

Jinyao Liu [a], Yan Pang [b,*], Jun Chen [c], Ping Huang [a], Wei Huang [a,*], Xinyuan Zhu [b], Deyue Yan [a,*]

[a] School of Chemistry and Chemical Technology, Shanghai Jiao Tong University, 800 Dongchuan Road, Shanghai 200240, China
[b] State Key Laboratory of Metal Matrix Composites, Shanghai Jiao Tong University, 800 Dongchuan Road, Shanghai 200240, China
[c] Research Institute of Micro/Nano Science and Technology, Shanghai Jiao Tong University, 800 Dongchuan Road, Shanghai 200240, China

ARTICLE INFO

Article history:
Received 21 June 2012
Accepted 1 July 2012
Available online 17 July 2012

Keywords:
Polydiselenide
Hyperbranched
Anticancer agent
Self-delivery
Broad spectrum

ABSTRACT

This work presents a highly efficient, broad spectrum and self-delivery anticancer agent, which is the hyperbranched polydiselenide (HPSe) consisting of alternative hydrophobic diselenide groups and hydrophilic phosphate segments in the backbone framework. The data of systematic evaluations demonstrate that HPSe is very potent to inhibit the proliferation of many forms of cancer cell. The dose of HPSe required for growth inhibition of 50% (IC_{50}) in all of the tested cancer cell lines is within the concentration range between 1 and 2.5 μg mL^{-1} with the incubation time of 72 h. Furthermore, the amphiphilic HPSe can self-assembly into nanomicelles with an average diameter of 50 nm and spontaneously enter into tumor cells by the enhanced permeability and retention (EPR) effect. Besides, other hydrophobic anticancer drugs such as doxorubicin (DOX) can be encapsulated into HPSe micelles for combining therapy.

1. Introduction

Up to date, great efforts have been paid to the synthesis of potent anticancer drugs and their prodrugs, respectively [1–3]. Prodrugs made of hydrophobic anticancer drugs with a hydrophilic polymer (for instance, polyethylene glycol) delivered into tumor cells with more effective cancer treatment [4–8]. However, the polymer itself has no direct therapeutical effect, and its metabolites might lead to unexpected side effects, such as toxicity and inflammation [9]. It would be significant to search a highly efficient, broad spectrum and self-delivery drug for cancer therapy. This work synthesized a macromolecular anticancer agent consisting of alternative hydrophobic diselenide and hydrophilic phosphate groups in the dendritic backbone. Interestingly, this polydiselenide exhibits a very potent anticancer effect in a broad spectrum. Benefiting from its amphiphilicity, the obtained macromolecular anticancer agent can self-assemble into nanomicelles, and then self-deliver into tumor cells through the enhanced permeability and retention (EPR) effect [10].

During last decades, selenium compounds have been proved to be a category of good anticancer agents because of their remarkable ability to enhance the immune response and produce anticancer metabolites which can efficiently perturb cancer cell metabolism, inhibit angiogenesis and induce apoptosis of cancer cells [11–18]. A great number of selenium compounds including inorganoselenium and organoselenium compounds have been reported as anticancer agents [19–21]. However, previous work in this research area focused on the design and synthesis of small-molecular-weight selenium drugs, probably due to the limited solubility and poor stability of the macromolecular selenium compounds.

Macromolecular compounds, such as proteins, genes, antibodies, peptides, oligonucleotides and some special synthetic polymers, have emerged as efficient medicines for various types of human diseases [22–27], and this research field has grown exponentially in recent years [28–31]. Due to the existence of many binding entities per molecule, macromolecular drugs exhibit multivalent interactions which can be found throughout the biological systems and can lead to a synergistic enhancement of a certain activity compared to the corresponding monomeric interaction [32]. It has been demonstrated that macromolecular drugs possess highly efficient and special pharmaceutical properties not found in small-molecular-weight drugs. Furthermore, their high-molecular-weight characteristics make them systemically non-absorbed, providing many advantages over small-molecular-weight drugs, for example, the long-term safety profiles. Therefore, the synthesis and application of macromolecular selenium anticancer agents would provide a favorable platform to develop potent drugs for cancer therapy. Last year we reported the

* Corresponding authors. Tel.: +86 2154742665; fax: +86 2154741297.
E-mail addresses: py-1985@sjtu.edu.cn (Y. Pang), hw66@sjtu.edu.cn (W. Huang), dyyan@sjtu.edu.cn (D. Yan).

0142-9612/$ – see front matter © 2012 Elsevier Ltd. All rights reserved.
http://dx.doi.org/10.1016/j.biomaterials.2012.07.003

preparation of the hyperbranched polydisulfide (HPS) through self-condensing ring opening polymerization, which is a smart redox-responsive drug carrier without any therapeutic activity for anti-cancer therapy [33]. In present work, we synthesized the hyperbranched polydiselenide (HPSe) through (A_2 + B_3) type polycondensation, which is an extensively efficient anticancer agent. The systematic evaluations of HPSe, i.e., the cytotoxicity effect, the cancer cell proliferation inhibition and the related apoptosis mechanism, were well performed. Meanwhile, the self-assembly of HPSe in water as well as the self-delivery and co-delivery of other drugs such as doxorubicin (DOX) for combining therapy were investigated carefully.

2. Materials and experimental methods

2.1. Materials

Chloroform and methylene chloride were dried by refluxing with calcium hydride and distilled just before use. Triethylamine (TEA) was refluxed with phthalic anhydride, potassium hydroxide, and calcium hydride in turn and distilled just before use. Tetrahydrofuran (THF) was dried by refluxing with the fresh sodium–benzophenone complex under nitrogen and distilled just before use. Phosphorus oxychloride ($POCl_3$) was distilled just before use. Nile red, *p*-toluene sulfonylchloride (TsCl), glutathione (reduced) (GSH), 3-(4,5-dimethyl-thiazol-2-yl)-2,5-diphenyl tetrazolium bromide (MTT), 2-(4-amidinophenyl)-6-indolecarbamidine dihydrochloride (DAPI), Se powder, triethylene glycol (TEG), and sodium borohydride were purchased from Sigma and used as received. Doxorubicin hydrochloride (DOX·HCl) was purchased from Beijing Huafeng United Technology Corporation and used as received. Alexa fluor® 488 annexin V/dead cell apoptosis assay kit was purchased from Invitrogen and used as received. Bradford protein assay kit and caspase-3 activity assay kit were purchased from Beyotime Instituted of Biotechnology and used as received. Clear polystyrene tissue-culture-treated 12- and 96-well plates were obtained from Corning Costar. All other reagents and solvents were purchased from the domestic suppliers and used as received.

2.2. Measurements

Nuclear magnetic resonance (NMR) analyses were recorded on a Varian Mercury Plus 400 MHz spectrometer with deuterated chloroform ($CDCl_3$) as solvent. The number-average molecular weight (M_n), weight-average molecular weight (M_w), and M_w/M_n were measured by gel permeation chromatography (GPC). GPC was performed on a Perkin–Elmer series 200 system (10 μm PL gel 300 × 7.5 mm mixed-B and mixed-C column, linear polystyrene calibration) equipped with a refractive index (RI) detector. DMF containing 0.01 mol L^{-1} lithium bromide was used as the mobile phase at a flow rate of 1 mL min^{-1} at 70 °C. Fourier transform infrared spectrometer (FTIR) spectra were recorded on a Paragon 1000 instrument by KBr sample holder method. Differential scanning calorimeter (DSC) was performed on a Perkin–Elmer Pyris 1 in nitrogen atmosphere. Both In and Zn standards were used for temperature and enthalpy calibrations. First, all the samples (about 5.0 mg in weight) were heated from room temperature to 150 °C, held at this temperature for 3 min to remove the thermal history and quenched to −80 °C. The samples were heated from −80 °C to 150 °C at 10 °C min^{-1} to determine the glass transition temperature (T_g). Dynamic light scattering (DLS) measurements were performed in aqueous solution using a Malvern Zetasizer Nano S apparatus equipped with a 4.0 mW laser operating at λ = 633 nm. The samples of 0.25 mg mL^{-1} were measured at 20 °C and at a scattering angle of 173°. Transmission electron microscopy (TEM) studies were performed with a JEOL 2010 instrument operated at 200 kV. The samples were prepared by directly dropping the solution of micelles onto carbon-coated copper grids. The samples were frozen by liquid nitrogen quickly and lyophilized by a freeze-dryer system (Martin Christ, α1-4) at −20 °C overnight before measurement.

2.3. Synthetic procedures

2.3.1. Synthesis of 2-(2-(2-hydroxyethoxy)ethoxy)ethyl 4-methylbenzenesulfonate

In a typical procedure: TsCl (49.57 g, 0.26 mol) in 100 mL of methylene chloride was added dropwise over 2 h to a solution of TEG (195 g, 1.5 mol) and TEA (26.26 g, 0.26 mol) in 100 mL of methylene chloride at 0 °C. Then, the solution was stirred overnight at room temperature. The organic layer was washed with saturated $NaHCO_3$ solution and dried over anhydrous $MgSO_4$. After the evaporation of solvent, the crude product was purified by flash column chromatography (SiO_2, chloroform/methanol 98:2) to yield a colorless oil, yield 62%. ^{1}H NMR ($CDCl_3$, ppm): 7.80 (2H, ArH), 7.34 (2H, ArH), 4.17 (2H, OCH_2CH_2OTs), 3.71 (2H, OCH_2CH_2OTs), 3.61 (4H, OCH_2CH_2O), 3.57 (2H, OCH_2CH_2OH), 2.44 (3H, $ArCH_3$). The ^{1}H NMR spectrum of 2-(2-(2-hydroxyethoxy)ethoxy)ethyl 4-methylbenzenesulfonate was shown in Fig. S1.

2.3.2. Synthesis of NaSeSeNa

The chemical equation is shown below:

$$2\ NaBH_4 + 2\ Se + 6\ H_2O \rightarrow NaSeSeNa + 2\ H_3BO_3 + 7\ H_2\uparrow$$

In a typical procedure: Sodium borohydride (4.921 g, 130 mmol) in 50 mL of water was added with magnetic stirring to selenium (5.132 g, 65 mmol) suspended in 50 mL of water at room temperature. After the initial vigorous, reaction had subsided (20 min), and additional equiv of selenium (5.132 g, 65 mmol) was added. The mixture was stirred for 10 min and then warmed briefly to dissolve selenium. The resulting brownish red aqueous solution of NaSeSeNa was then ready for further use.

2.3.3. Synthesis of 2-(2-(2-hydroxyethoxy)ethoxy)ethyl diselenide

In a typical procedure: NaSeSeNa (65 mmol) solution was added with magnetic stirring to 300 mL of THF solution of 2-(2-(2-hydroxyethoxy)ethoxy)ethyl 4-methylbenzenesulfonate (39.562 g, 130 mmol) with nitrogen protection. The mixture was stirred for 48 h at 50 °C. Then, the solvent was removed, and the crude product was redissolved in methylene chloride. The organic layer was washed twice with water and then dried over anhydrous $MgSO_4$. The product was purified by silica gel column chromatography eluting with 1:1 hexane/ethyl acetate. The evaporation of solvent gave a brown oil product, yield 65%. ^{1}H NMR ($CDCl_3$, ppm): 3.77 (4H, $SeCH_2CH_2O$), 3.72 (4H, OCH_2CH_2OH), 3.67 (4H, $OCH_2CH_2OCH_2CH_2OH$), 3.65 (4H, $OCH_2CH_2OCH_2CH_2OH$), 3.59 (2H, OCH_2CH_2OH), 3.12 (4H, $SeCH_2CH_2O$). ^{77}Se NMR ($CDCl_3$, ppm): 289.20. The (a) ^{1}H NMR and (b) ^{77}Se NMR spectra of 2-(2-(2-hydroxyethoxy)ethoxy)ethyl diselenide were shown in Fig. S2.

2.3.4. Synthesis of hyperbranched polydiselenide

In a typical procedure: 20 mL of chloroform solution of 2-(2-(2-hydroxyethoxy) ethoxy)ethyl diselenide (2.12 g, 5.00 mmol) and TEA (0.841 g, 8.33 mmol) was added to a 50 mL round-bottomed flask with nitrogen protection. A mixture of $POCl_3$ (0.426 g, 2.78 mmol) and 5 mL of chloroform was slowly added to the above flask at 0 °C using an ice bath and then kept at room temperature for 24 h. The by-product of triethylamine hydrochloride salt was removed by filtration. The obtained filtrate was twice extracted by HCl (1 M), $NaHCO_3$ (10%) and NaCl (saturated) aqueous solution, respectively. After drying over anhydrous $MgSO_4$, the solvent was removed under vacuum, obtaining a brown solid product, named HPSe, 72% yield. ^{1}H NMR ($CDCl_3$, ppm): 4.19 (2H, $POCH_2CH_2O$), 3.76 (4H, OCH_2CH_2Se), 3.72 (2H, OCH_2CH_2OH), 3.65 (12H, $POCH_2CH_2O$, $OCH_2CH_2OCH_2CH_2OH$), 3.10 (4H, $SeCH_2CH_2O$). ^{31}P NMR ($CDCl_3$, ppm): 1.27 (P in dendritic units), 0.16 (P in linear units), −11.72 (P in terminal units) [34]. ^{77}Se NMR ($CDCl_3$, ppm): 290.44. The FTIR spectrum and DSC curve of HPSe were shown in Fig. S3.

2.4. Cytotoxicity measurement

2.4.1. Cell culture

L929 cell (a murine fibroblasts cell line), NIH-3T3 cell (a mouse embryonic fibroblast cell line), HeLa cell (a human cervical carcinoma cell line), Cal-27 cell (a human head and neck squamous carcinoma cell line), HN-6 cell (a human primary squamous carcinoma of tongue cell line), MCF-7 cell (a human breast adenocarcinoma cell line), and Bel-7402 cell (a human hepatocellular carcinoma cell line) were cultured in DMEM. MGC-803 cell (a human gastric carcinoma cell line) and 95-D cell (a highly metastatic lung carcinoma cell line) were cultivated in RPMI-1640. LoVo cell (a human colon carcinoma cell line) was cultured in F-12K. MDA-MB-231 cell (a human breast adenocarcinoma cell line) was cultured in L-15. The culture mediums contain 10% FBS (fetal bovine serum) and antibiotics (50 units/mL penicillin and 50 units/mL streptomycin). MDA-MB-231 cells were incubated at 37 °C under a non–CO_2–equilibrated humidified atmosphere. The other cells were incubated at 37 °C under a humidified atmosphere containing 5% CO_2.

2.4.2. MTT assay

The cells were seeded into 96-well plates at 8 × 10^3 cells per well in 200 μL of culture medium. After 12 h of incubation, the medium was removed and replaced with another 200 μL of culture medium containing serial dilutions of HPSe or HPS from 0.25 to 25 μg mL^{-1}. HeLa cells without the treatment were used as control. The cells were grown further for different incubation times from 6 to 72 h. Then, 20 μL of 5 mg mL^{-1} MTT assay stock solution in PBS was added to each well. After the cells were incubated for 4 h, the medium containing unreacted MTT was carefully removed. Then, the obtained blue formazan crystals were dissolved in 200 μL $well^{-1}$ DMSO, and the absorbance was measured in a BioTek Synergy H4 hybrid reader at a wavelength of 490 nm. The blank was subtracted to the measured optical density (OD) values, and the cell viability was expressed as % of the values obtained for the untreated control cells.

2.4.3. Apoptosis assay

HeLa cells were seeded in six-well plates at 5 × 10^5 cells per well in 1 mL of complete DMEM and cultured for 12 h, followed by removing culture medium and adding 1 mL HPSe solution of DMEM at various concentrations from 0.25 to 25 μg mL^{-1}. HeLa cells without the incubation of HPSe were used as control. After 12 h incubation, cells were rinsed by PBS twice and treated with trypsin. Then, 2 mL

of cold PBS was added to each culture well, and the solutions were centrifugated at 1000 rpm for 5 min at 4 °C. After the removal of supernatants, the cells were resuspended in 1X annexin-binding buffer at about 1×10^6 cells mL^{-1}. Then, 5 μL of Alexa Fluor® 488 annexin V and 1 μL of 100 μg mL^{-1} PI working solutions were added to each 100 μL of the cell suspension. After 15 min incubation at room temperature, 400 μL of 1X annexin-binding buffer was added. The samples were kept on ice and analyzed by flow cytometry. Data for 5000 gated events were collected, and the analysis of live and dead cells was performed by means of a BD FACSCalibur flow cytometer and CELLQuest software. In confocal laser scanning microscopy (CLSM) measurements, the cells were further fixed with 4% formaldehyde for 30 min at room temperature, and the slides were rinsed with PBS for three times. The slides were mounted and observed by an LSM 510META.

2.5. Caspase-3 activity

2.5.1. Caspase-3 protein activity assay

HeLa cells were seeded in six-well plates at 1.0×10^6 cells per well in 1 mL of complete DMEM and cultured for 12 h, followed by removing the culture medium and adding 1 mL HPSe solution of DMEM at various concentrations from 0.25 to 10 μg mL^{-1}. HeLa cells without the incubation of HPSe were used as control. After 12 h incubation, cells were rinsed by PBS twice and treated with trypsin. Then, 2 mL of cold PBS was added to each well, and the solutions were centrifugated at 1000 rpm for 5 min at 4 °C. After the removal of supernatants, the cells were resuspended in 100 μL of lysate and kept on ice for 15 min. Lysates were transferred in micro-centrifuge tubes and centrifuged at 12,000 rpm for 10 min at 4 °C. The protein content in the supernatant was determined by Bradford protein assay and then adjusted to the same concentration. 90 μL of the protein solution were distributed in each well of a 96-well plate, and 10 μL of the Ac-DEVD-*p*NA caspase-3 substrate was added to reach a final concentration of 200 μM. The absorbance at 405 nm was read after 2 h of incubation at 37 °C with a BioTek Synergy H4 hybrid reader at a wavelength of 405 nm. The blank was subtracted to the measured OD values, and the activity was expressed as fold of the values obtained for the untreated control cells.

2.5.2. Caspases-3 mRNA expression level assay

HeLa cells were seeded in six-well plates at 1.0×10^6 cells per well in 1 mL of complete DMEM and cultured for 12 h, followed by removing the culture medium and adding 1 mL HPSe solution of DMEM at various concentrations from 0.25 to 10 μg mL^{-1}. HeLa cells without the incubation of HPSe were used as control. After 12 h incubation, cells were rinsed by PBS twice and treated with trypsin. Total cellular RNA in the treated or control cells were isolated by RNeasy kit (Qiagen) according to the manufacturer's instructions. About 1 mg of total RNA was used for reverse transcription by using a one-step real-time quantitative reverse transcription polymerase chain reaction (RT-PCR) kit (Invitrogen) in a thermocycler (Bio-rad iQ5, Bio-rad) under the following reaction conditions: cDNA synthesis, 45 °C for 30 min; inactivation, 94 °C for 2 min; PCR amplification of 40 cycles, denature at 94 °C for 30 s, annealing at 60 °C for 30 s, chain extension at 72 °C for 45 s, and a final chain extension at 72 °C for 10 min. Caspase-3 primer sequences were 5′-TGTCATCTCGCTCTGGTACG-3′ (forward) and 5′-AAATGACCCCTTCATCACCA-3′ (reverse) [35]. As an internal control, glyceraldehyde-3-phosphatedehydrogenase (GAPDH) was amplified using primer sequences 5′-AACTTTGGCATTGTGGAAGG-3′ (forward) and 5′-GGAGACAACCTGGTCCTCAG-3′ (reverse). The expression of caspase-3 in experimental samples was determined by the comparative Ct method ($2^{-(\Delta)(\Delta)Ct}$ method), in which Ct is the threshold cycle and ΔΔCt = (ΔCt caspase-3) − (ΔCt reference RNA (GAPDH)).

2.6. Preparation and reduction-triggered drug release of HPSe micelles

2.6.1. Preparation of HPSe self-assembled micelles

In brief, 10 mg HPSe was dissolved in 2 mL of DMF and stirred at room temperature for 0.5 h. Then, the solution was slowly added to 5 mL of deionized water and stirred for another 0.5 h. Subsequently, the solution was dialyzed against deionized water for 24 h (MWCO = 15,000 g mol^{-1}), and the deionized water was exchanged every 4 h. Water is the good solvent for phosphate groups and the nonsolvent for diselenide groups. The appearance of turbidity in the aqueous solution indicated the formation of aggregations.

2.6.2. Critical aggregation concentration measurement

Pyrene was used as the fluorescence probe to investigate the critical aggregation concentration of HPSe. Firstly, HPSe was dissolved in the aqueous solution of pyrene. Then, the solution was diluted to various desired concentrations (from 1 mg mL^{-1} to 1.0×10^{-5} mg mL^{-1}) with a constant pyrene concentration of 6.0×10^{-7} mol L^{-1}. The fluorescence spectra of all solutions were recorded on an LS-50B luminescence spectrometer (Perkin Elmer Co.). The excitation wavelength was set at 335 nm. The I_3/I_1 ratio values of all solutions were recorded.

2.6.3. Preparation of Nile red or DOX-loaded HPSe micelles

In a typical procedure for the preparation of Nile red or DOX-loaded HPSe micelles [33]: 20 mg HPSe was dissolved in 2 mL of DMF, followed by the addition of a predetermined amount of DOX·HCl (2 M equivalents of triethylamine should be added) or Nile red, and stirred at room temperature for 2 h. Then, the mixture was slowly added to 5 mL of deionized water and stirred for another 2 h. Subsequently, the solution was dialyzed against deionized water for 24 h (MWCO = 15,000 g mol^{-1}), and the deionized water was exchanged every 4 h.

To determine the total loading of drug, the DOX-loaded micelle solution was lyophilized and then dissolved in DMF again. The UV absorbance of the solution at 500 nm was measured to determine the total loading of DOX. Drug loading content (DLC) and drug loading efficiency (DLE) were calculated according to the following formula

$$\text{DLC (wt\%)} = (\text{weight of loaded drug/weight of polymer}) \times 100\%$$
$$\text{DLE (\%)} = (\text{weight of loaded drug/weight in feed}) \times 100\%$$

When the feed ratio of polymer to DOX was 20:1, the DLC and DLE of HPSe micelles were determined to be 3.08% and 61.6% respectively.

2.6.4. Reduction-triggered drug release

The experiments of reduction-triggered intracellular drug release were performed on CLSM measurements [36]. HeLa cells were seeded in six-well plates at 2×10^5 cells per well in 1 mL of complete DMEM and cultured for 12 h and then incubated for additional 3 h with DOX-loaded HPSe micelles at a final DOX concentration of 0.8 μg mL^{-1} in complete DMEM. Free DOX and DOX-loaded PEG-*b*-PCL micelles were both used as control. Then, the culture medium was removed, and cells were washed with PBS three times. Thereafter, the cells were fixed with 4% formaldehyde for 30 min at room temperature, and the slides were rinsed with PBS for three times. Finally, the cell nuclei were stained with DAPI for 10 min, and the slides were rinsed with PBS for three times. The slides were mounted and observed by an LSM 510META.

3. Results and discussion

3.1. Synthesis and characterization of HPSe

Only a few successful examples have been shown, hitherto, for the synthesis of diselenide-containing polymers, because these systems generally involve in a low solubility and poor stability of the polymer [37–39]. Hyperbranched polymers have demonstrated some special characteristics, such as the three dimensional globular architecture, non-entanglement, better solubility and so forth [40–44]. Therefore, the hyperbranched polymer with a number of diselenide bonds inside may possess a good solubility and better stability. The diselenide moiety was introduced into a diol intermediate. Then the hyperbranched polyselenide was synthesized via the polymerization of the diselenide-containing diol (in a slight excess) with phosphorus oxychloride under an alkalescent environment. The resulting HPSe has a highly branched structure with alternative diselenide and phosphate groups in its backbone framework (Scheme 1). Polyphosphate was used as the basic component of HPSe because of its excellent biocompatibility and biodegradability [45,46]. As expected, HPSe has a good solubility and stability in common solvents. The resulting HPSe was characterized by NMR, FTIR, DSC and GPC instruments.

Typical ^1H, ^{31}P, and ^{77}Se NMR spectra of HPSe are shown in Fig. 1. According to ^1H NMR spectrum in Fig. 1a, the resonances at 4.19, 3.76, 3.72, 3.65, and 3.10 ppm are assigned to the methylene protons of $POCH_2CH_2O$, OCH_2CH_2Se, OCH_2CH_2OH, $POCH_2CH_2O$/$OCH_2CH_2OCH_2CH_2OH$, and $SeCH_2CH_2O$, respectively. The corresponding signals of phosphorus atoms of HPSe are labeled in Fig. 1b. The peaks at 1.27, 0.16, and −11.72 ppm are attributed to the phosphorus atoms in dendritic, linear, and terminal units of HPSe, respectively. The degree of branching (DB) of the resulting HPSe is 0.44 according to the quantitative ^{31}P NMR spectrum [47]. The peak at 290.44 ppm in the ^{77}Se NMR spectrum of HPSe is the resonance of diselenide groups (Fig. 1c). Furthermore, the FTIR spectrum and DSC curve of HPSe are shown in Fig. S3. The absorptions at 1263, 1178 and 986 cm^{-1} are attributed to the asymmetrical, symmetrical stretching of P═O and P–O–C, respectively. The peak at 3435 cm^{-1} is assigned to the large number of terminal hydroxyl groups. DSC curve shows that the T_g of HPSe is located at −45 °C. Moreover, the

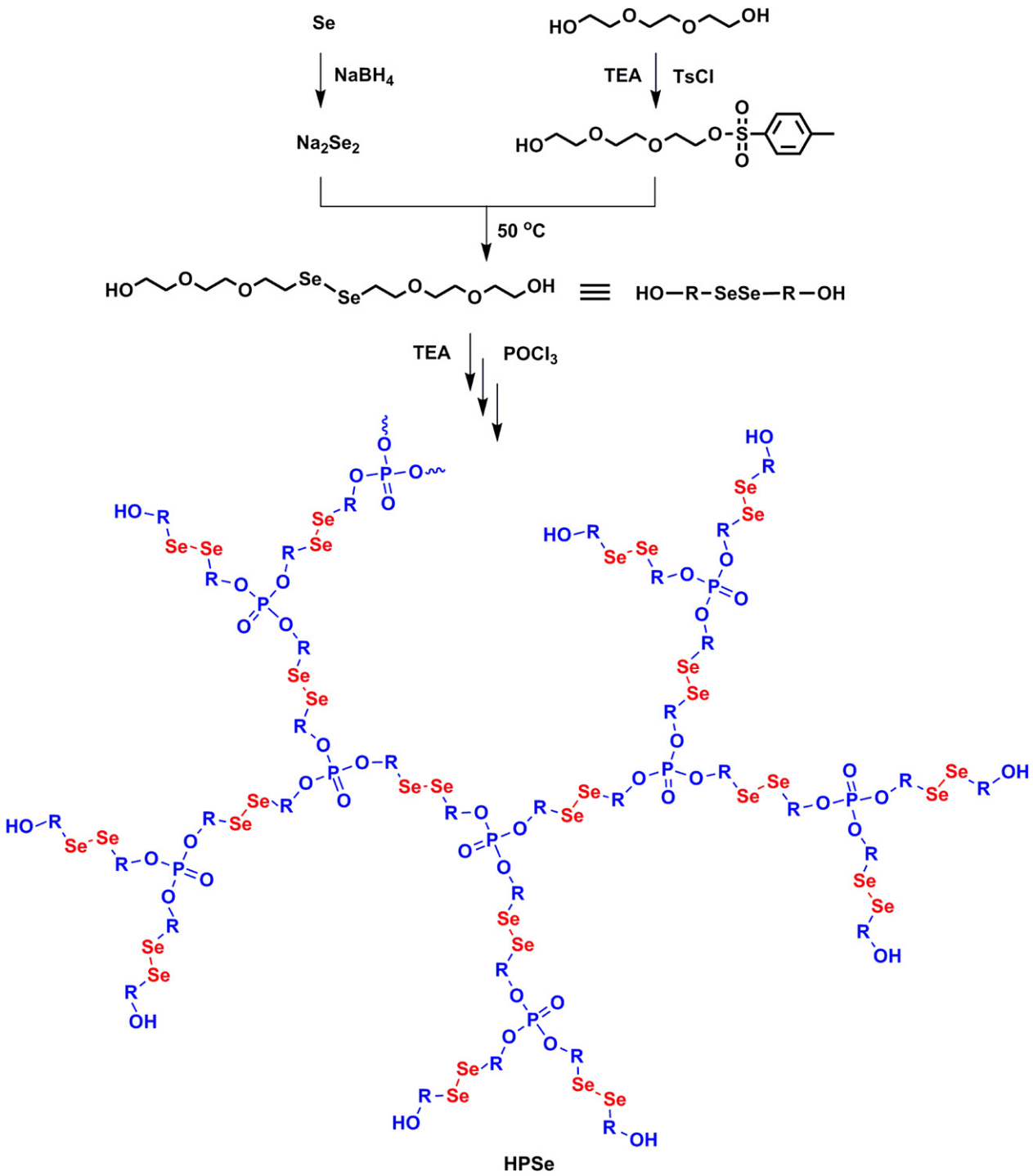

Scheme 1. Detailed synthetic route of HPSe.

weight-average molecular weight of HPSe characterized by GPC is 6100 g mol^{-1} with the polydispersity index of 1.7. These results well demonstrate the successful synthesis of HPSe.

3.2. *In vitro cytotoxicity of HPSe*

The cytotoxicity effects of HPSe were examined in two normal cell lines (L929 cells and NIH-3T3 cells) by using a standard MTT assay. Cells were first cultured overnight for adherence and then treated with HPSe at various concentrations from 0.25 to 2.5 μg mL^{-1} for 6 and 12 h respectively. The cells without treatment of HPSe were used as control. It was found that no evident cell proliferation inhibition was induced by HPSe in these two cell lines in the test concentration range after 6 h incubation (Fig. 2). With increasing the incubation time to 12 h, HPSe only induced a limited decrease of cell viability (<10%) at the concentration up to 2.5 μg mL^{-1}, indicating the low cytotoxicity of HPSe against normal cells. However, viabilities of human cancer cells were significantly reduced when the cells were treated with HPSe under the same conditions. After 6 h of incubation, the viability of cervical carcinoma cell line HeLa was decreased to 73% at the concentration of HPSe up to 2.5 μg mL^{-1}. With the increase of incubation time to

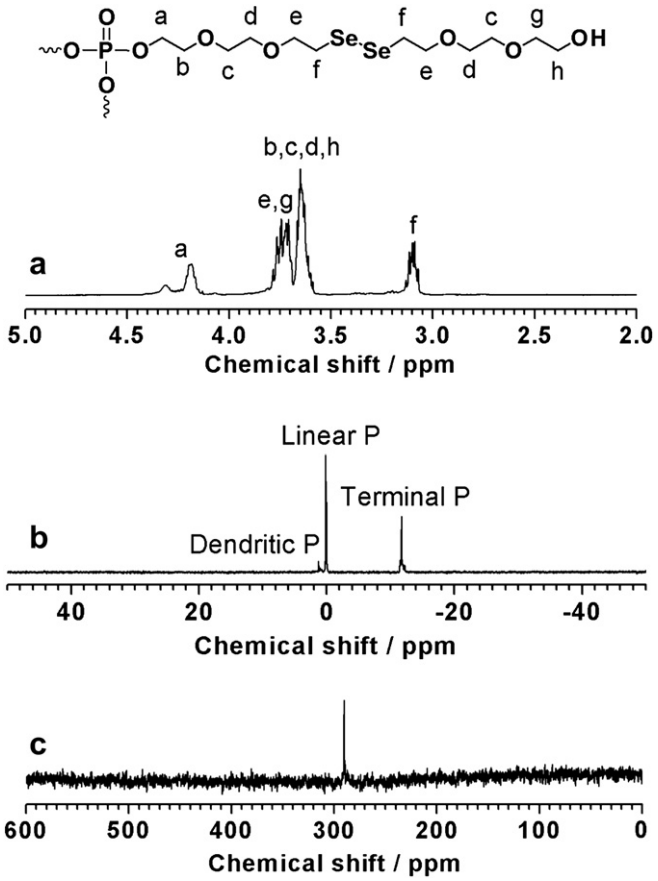

Fig. 1. (a) ^{1}H NMR, (b) ^{31}P NMR and (c) ^{77}Se NMR spectra of HPSe in $CDCl_3$.

12 h, the viability of HeLa cells was further reduced to 64%. It has been reported that a selective mechanism of selenium makes cancer cells prone to undergo apoptosis, while normal non-cancer cells remain unaffected [48]. Therefore, the difference in cell viability between normal cells and cancer cells can be ascribed to the anticancer action of HPSe. Namely, HPSe specifically inhibits the proliferation of cancer cells, but induces no evident toxicity effects on the viability of normal cells.

3.3. *In vitro anticancer effect of HPSe*

The anticancer abilities of HPSe were systematically tested in vitro in a series of human cancer cell lines. Typically, cells were first cultured overnight for adherence and then incubated with HPSe at different concentrations from 0.25 to 25 μg mL^{-1} for 24, 48 and 72 h, respectively. The cells without treatment of HPSe were used as control. It was observed that HPSe exhibited highly efficient abilities of proliferation inhibition in all of the tested human cancer cells. Meanwhile, HPSe inhibited the proliferation of cancer cells in a dose- and time-dependent fashion (Fig. 3). After 24 h incubation, the dose of growth inhibition of 50% (IC_{50}) was observed in the concentration range between 2.5 and 5 μg mL^{-1} in colon carcinoma cell line LoVo, primary squamous carcinoma of tongue cell line HN-6, breast adenocarcinoma cell line MDA-MB-231, highly metastatic carcinoma cell line 95-D, head and neck squamous carcinoma cell line Cal-27 and breast adenocarcinoma cell line MCF-7. The dose of IC_{50} was shown in a slightly elevated concentration range between 5 and 10 μg mL^{-1} in gastric carcinoma cell line MGC-803, cervical carcinoma cell line HeLa and hepatocellular carcinoma cell line Bel-7402. Interestingly, with increasing the incubation time to 72 h, the dose of HPSe required for IC_{50} in all of the tested cells significantly

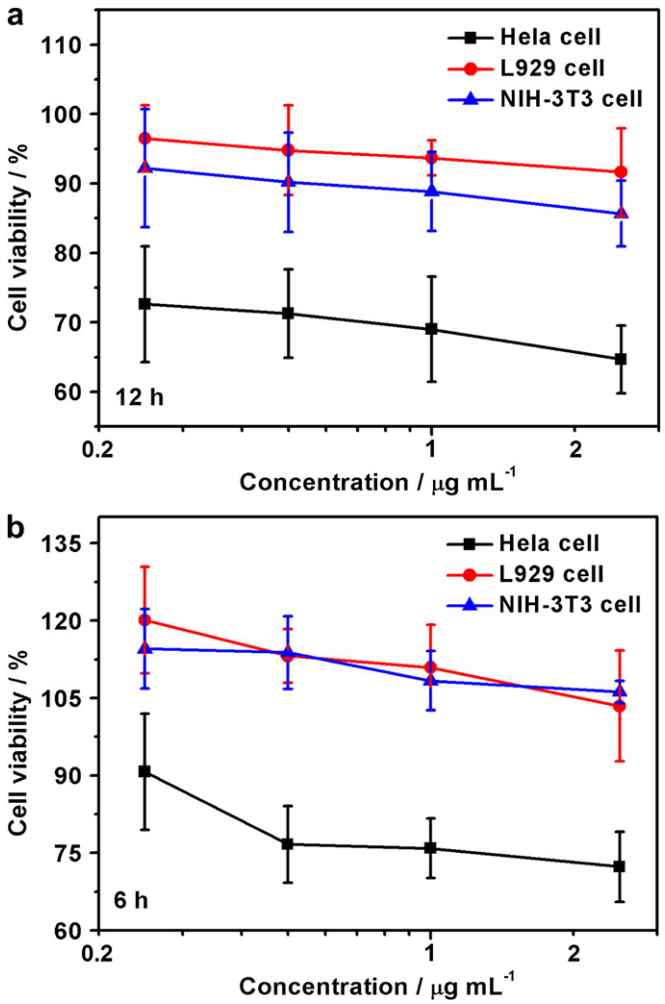

Fig. 2. Cell viabilities of mouse fibroblasts cell line L929, mouse embryonic fibroblast cell line NIH-3T3 and human cervical carcinoma cell line HeLa incubated with HPSe at various concentrations from 0.25 to 2.5 μg mL^{-1} for (a) 6 h and (b) 12 h respectively. The cells without the treatment of HPSe were used as controls. The data are presented as average ± standard deviation ($n = 6$).

decreased to the concentration range between 1 and 2.5 μg mL^{-1}. HPSe displayed markedly improved abilities of proliferation inhibition in human cancer cells compared to the conventional small-molecular-weight selenium anticancer agents. It has been reported that one of the most potent derivatives of benzisoselenazolone (a representative alkyl aryl selenide anticancer agent) has the IC_{50} values of 42.7 and 10.6 μg mL^{-1} in HeLa cells and Bel-7402 cells respectively [49]. The results given above confirm the highly efficient and broad spectrum nature of HPSe to inhibit the proliferation of human cancer cells.

We speculated that the strongly enhanced anticancer abilities of HPSe might be attributed to the synergistic effect of diselenide groups distributed along the dendritic framework. In our previous report, a sulfur analog of HPSe (disulfide-containing hyperbranched polyphosphate, HPS) was synthesized as a biocompatible drug carrier [33]. Because of its redox and enzyme dual responsibility, HPS is excellent in drug delivery. However, it shows no therapeutical effect in anticancer therapy. In this work, the proliferation inhibition of HPS against HeLa cells was further checked by using MTT assay. It reveals that HPS exhibits a very low cell proliferation inhibition against HeLa cells in the identical test concentration range of HPSe (Fig. S4). When the incubation time was extended to 72 h, the viability of HeLa cells still kept above 95% at the HPS

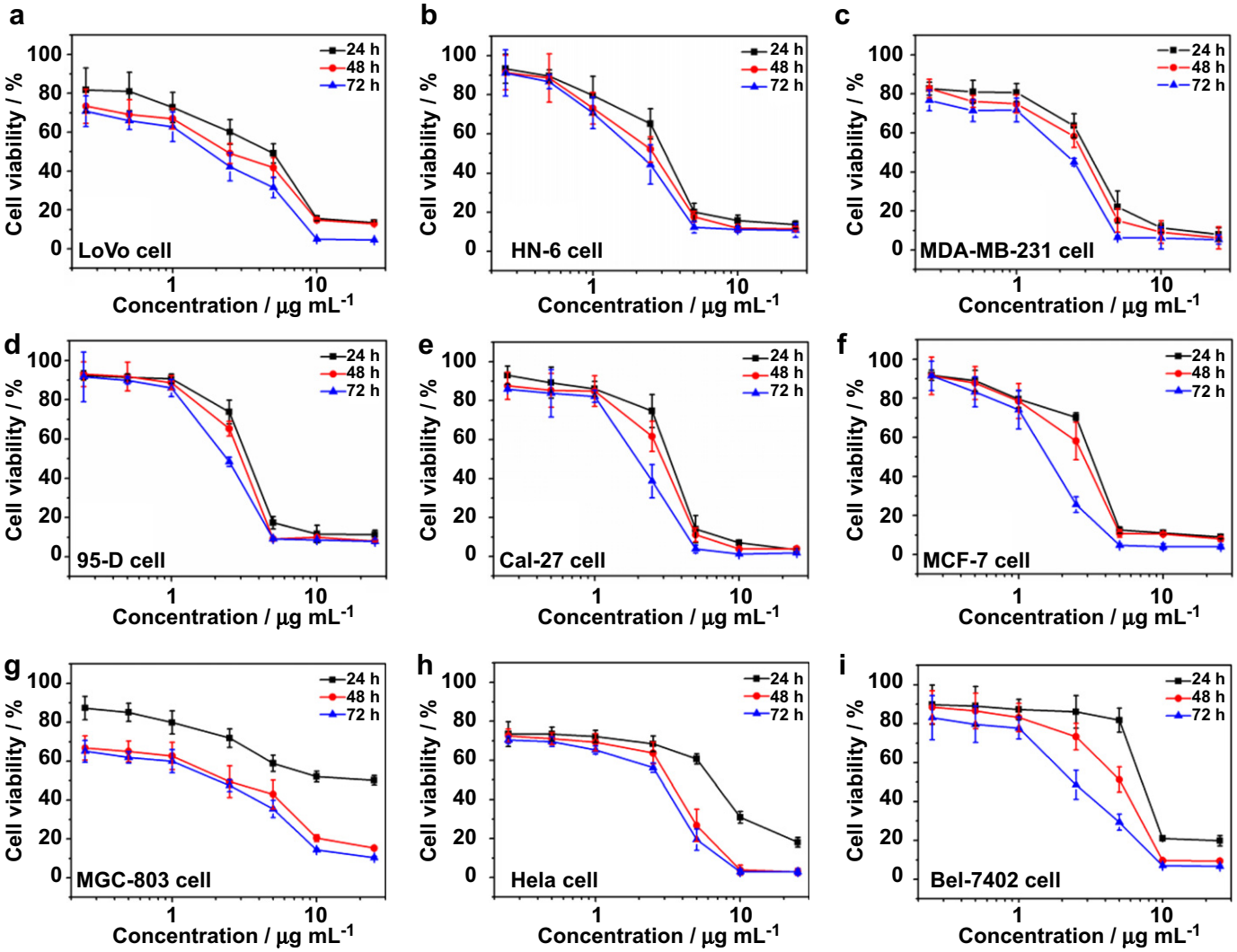

Fig. 3. Cell inhibitions of (a) LoVo cell, (b) HN-6 cell, (c) MDA-MB-231 cell, (d) 95-D cell, (e) Cal-27 cell, (f) MCF-7 cell, (g) MGC-803 cell, (h) HeLa cell and (i) Bel-7402 cell incubated with HPSe at various concentrations from 0.25 to 25 μg mL^{-1} for 24, 48 and 72 h, respectively. Cell viability was measured by MTT assay and the cells without the treatment of HPSe were used as controls. The data are presented as average ± standard deviation ($n = 6$).

concentration up to 25 μg mL^{-1}, suggesting no anticancer activity of HPS against HeLa cells. It is evident that the potent anticancer activities of HPSe come from diselenide groups.

3.4. Apoptosis of cancer cell induced by HPSe

It is known that selenium compound-induced cancer cell death is mainly apoptotic (programmed cell death). Here, FITC-Annexin V/propidium iodide (PI) method was used to verify whether the cancer cell death caused by HPSe was associated with apoptosis. HeLa cells were first incubated with HPSe at different concentrations from 0.25 to 25 μg mL^{-1} for 12 h and then subjected to FITC-Annexin V/PI staining. The cells without treatment of HPSe were used as control. Flow cytometry data show that HPSe is able to induce apoptosis in HeLa cells and the number of apoptotic cells increases in a dose-dependant manner (Fig. 4a and b). When exposed to 0.25 μg mL^{-1} of HPSe for 12 h, the ratio of apoptotic cells in whole tested HeLa cells reached to 34.74%. With the concentration of HPSe up to 25 μg mL^{-1}, the ratio of apoptotic cells dramatically increased to 99.16%. However, almost no apoptotic cells (<0.40%) were observed in the control cells. Furthermore, CLSM images show that the number of early apoptotic cells (green fluorescence of FITC-Annexin V) and late apoptotic cells (red fluorescence of PI) increased with the incubation concentration of HPSe (Fig. 4c). Both flow cytometry and CLSM data support our previous MTT analysis, confirming that HPSe can significantly induce apoptosis of human cancer cells.

Caspases are well known to be required for cell apoptosis induced by various stimuli. Among the caspase family members, caspase-3 is thought to be the main effector and has been identified as being activated in response to cytotoxic drugs [50]. The activation of caspase-3 is an important step in the execution phase of apoptosis and its inhibition blocks cell apoptosis. To better understand the mechanism of apoptosis triggered by HPSe in cancer cells, we wanted to know if the effector of caspases-3 was being activated to play a role in cell death. The caspase-3 protein activity and mRNA expression level in Hela cells were analyzed respectively by colorimetry using the substrate of Ac-DEVD-*p*NA and real-time quantitative reverse transcription polymerase chain reaction (RT-PCR) using the referred primers. The cells were treated with HPSe at different concentrations from 0.5 to 10 μg mL^{-1} for 12 h and the cells without treatment of HPSe were used as control. It was found that caspase-3 protein activity in HeLa cells increased upon the treatment of HPSe and showed a dose-dependent increase (Fig. 5a).

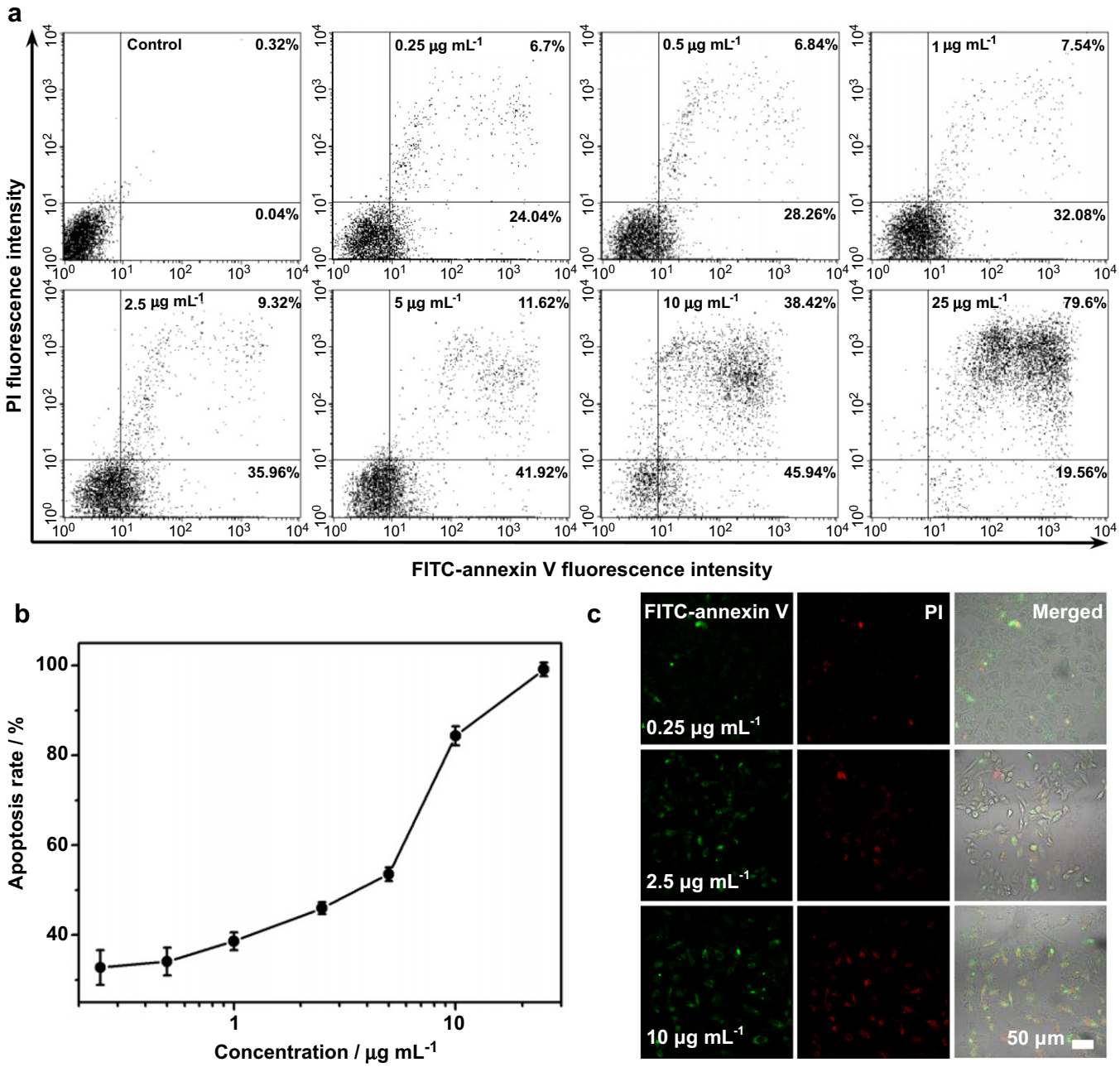

Fig. 4. (a) Representative flow cytometric analysis results of cell apoptosis of HeLa cells treated with HPSe at various concentrations from 0.25 to 25 μg mL^{-1} for 12 h. Lower left, living cells; Lower right, early apoptotic cells; Upper right, late apoptotic cells; Upper left, necrotic cells. Inserted numbers in the profiles indicate the percentage of the cells present in this area. (b) The relationship of incubation concentration of HPSe and ratio of apoptotic HeLa cells based on the results of flow cytometry measurements. The data are presented as average ± standard deviation ($n = 3$). (c) Representative CLSM images of HeLa cells incubated with HPSe for 12 h at the concentrations of 0.25, 2.5 and 10 μg mL^{-1}, respectively. The cells were stained by FITC-annexin V and PI.

After the cells incubated with HPSe for 12 h at the concentration of 0.5 μg mL^{-1}, the caspase-3 protein activity increased to 2.3-fold of the control cells. When the concentration increased to 10 μg mL^{-1}, the activity further increased to 4.5-fold of the control cells, suggesting the role of caspase-3 activation in HPSe-induced cancer cell death. Similar results of caspase-3 mRNA expression level were also obtained in HeLa cells (Fig. 5b). With increasing the concentration of HPSe from 0.5 to 10 μg mL^{-1}, the caspase-3 mRNA expression level remarkably increased from 1.8 to 22.8-fold of the control cells, further indicating this type of apoptosis was dependent on caspase-3 activity. In general, HPSe significantly induces the apoptosis of cancer cells in a dose-dependant manner and the apoptosis is based on the caspase-3 mechanism.

3.5. Self-assembly and GSH-responsiveness of HPSe micelles

Macromolecular drugs including proteins and genes often encounter several challenges, such as fast degradation in the physiological milieu, lack of targeting ability and inefficient translocation into the cell cytoplasm. Advancement in nanotechnology has now allowed for development of various efficient delivery systems. Polymer micelles are recognized as promising nanocarriers because of the unique advantages including the enhanced bioavailability of drugs, preferential accumulation at the tumor sites by EPR effect and efficient cell internalization [51]. HPSe is an amphiphilic macromolecule with alternative hydrophobic diselenide and hydrophilic phosphate groups in the highly branched

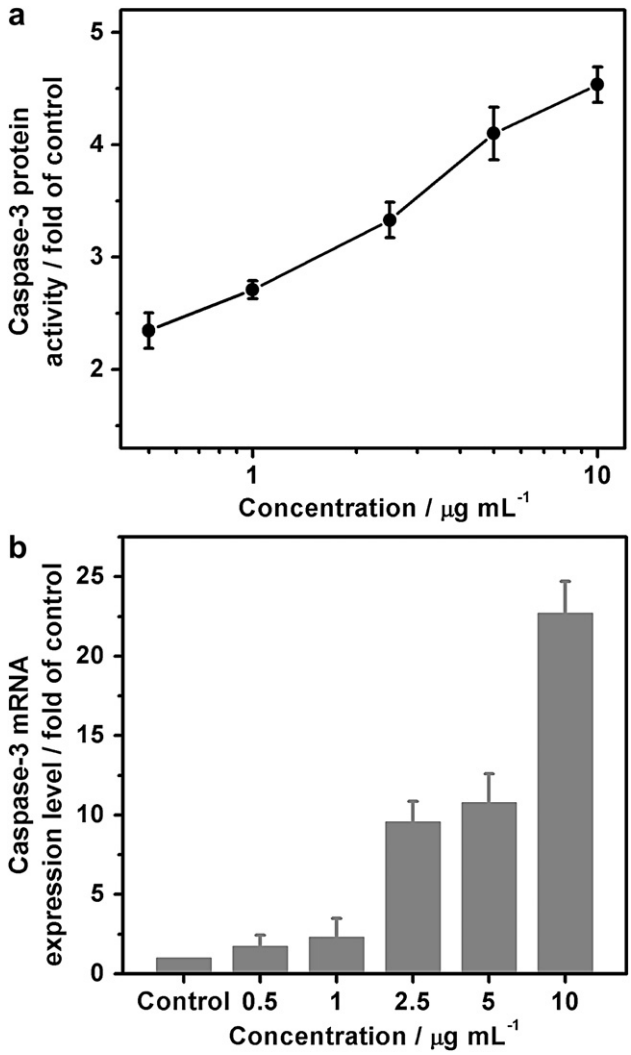

Fig. 5. (a) Caspase-3 protein activity in HeLa cells activated by HPSe at various concentrations from 0.5 to 10 μg mL^{-1} for 12 h. (b) Caspase-3 mRNA expression level of HeLa cells treated with HPSe at various concentrations from 0.5 to 10 μg mL^{-1} for 12 h. Cells without the treatment of HPSe were used as controls and the data are presented as average ± standard deviation ($n = 3$).

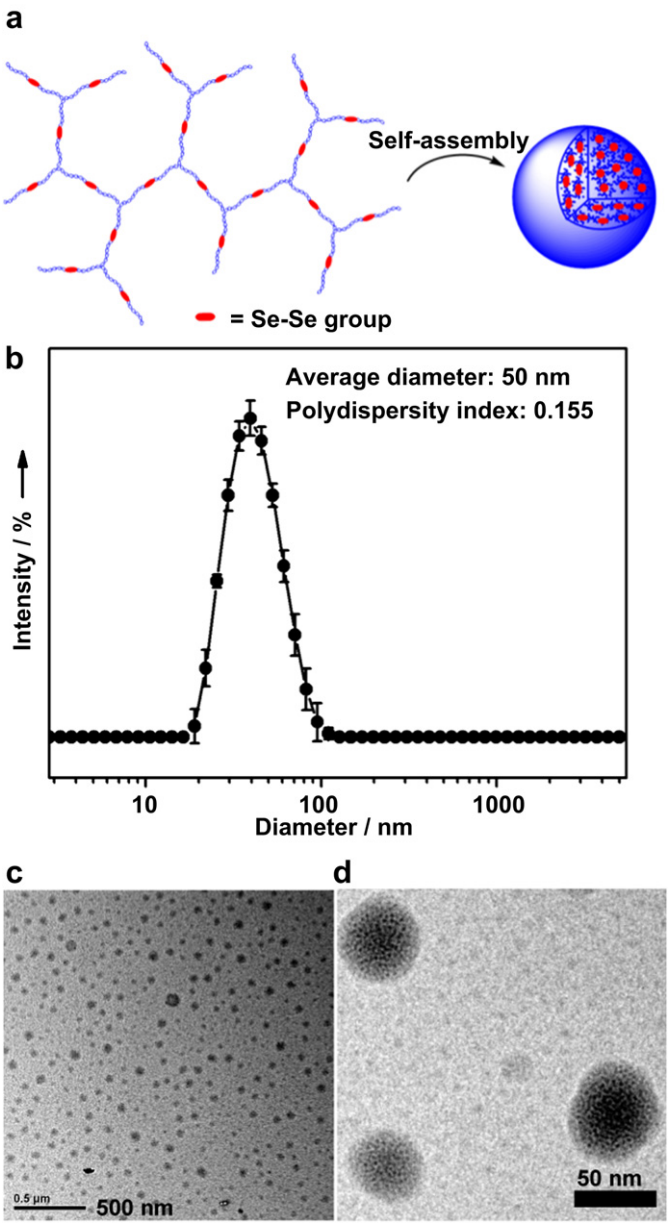

Fig. 6. (a) Schematic representation of self-assembly of HPSe in water and the multi-core/shell aggregating structure of resulting micelles. (b) Size and size distribution of HPSe micelles measured by dynamic light scattering (DLS). Data are presented as average ± standard deviation ($n = 3$). Representative TEM images of (c) HPSe micelles and (d) the unique multi-core/shell aggregating structure.

backbone, which can self-assemble into unique multi-core/shell spherical micelles in water with an average size of 50 nm and a critical aggregation concentration of 5 μg mL^{-1} (Fig. 6). The mutual repulsion stemming from the immiscibility of the two type groups drives the system to segregate and induces the microphase separation in water, forming the core/shell structure. Due to the limited sizes of the large amount of hydrophobic and hydrophilic groups in HPSe, it seems impossible to form a micelle of 50 nm with only one hydrophobic core. The enlarged TEM image clearly shows the micelle is composed of a lot of small black domains (attributed to the aggregated hydrophobic diselenide groups), and the hydrophobic micro-domains are surrounded by the continuous hydrophilic phase (attributed to the aggregated polyphosphate groups) (Fig. 6d). So the multi-core/shell structure of the micelle is formed. Meanwhile, HPSe micelles display a sensitive redox-responsiveness because of the existence of many diselenide groups. It was found that the fluorescence emission intensity of Nile red encapsulated inside HPSe micelles rapidly declined within 60 min in the presence of 10 mM GSH (Fig. 7a), while the micelles without GSH were remained unchanged, suggesting the fast destabilization of the micellar structure as well as the triggered release of dye molecules.

^{77}Se NMR spectrum further verified the cleavage of diselenide bonds under the reduction environment. The peak at 290.2 ppm assigned to the resonance of diselenide groups was reduced with increasing incubation time of GSH (Fig. 7b). On the other hand, the newly emerged peak at 286.5 ppm attributed to the signal of selenol groups was evidently grown, indicating the cleavage of diselenide bonds as well. Thus, the self-assembly and redox-responsiveness endow HPSe with the properties of self-delivery, co-delivery of other drugs and triggered drug release.

3.6. Self-delivery and co-delivery of HPSe micelles

As a model hydrophobic anticancer agent, DOX was encapsulated inside HPSe micelles with the drug loading content of 3.08% and the drug loading efficiency of 61.6%, respectively. The

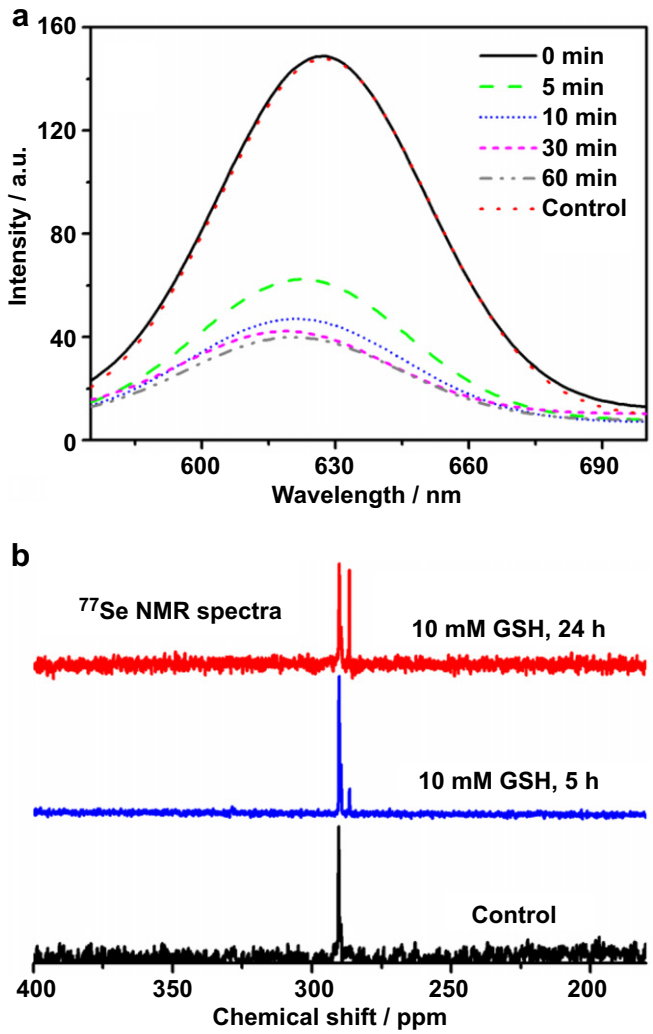

Fig. 7. (a) Change in fluorescence emission intensity of Nile red encapsulated inside HPSe micelles in the presence of 10 mM GSH at different time intervals. The sample without the presence of GSH was used as control. (b) Change in ^{77}Se NMR spectrum of HPSe in deuterated chloroform in the presence of 10 mM GSH at different time intervals. The sample without the presence of GSH was used as control.

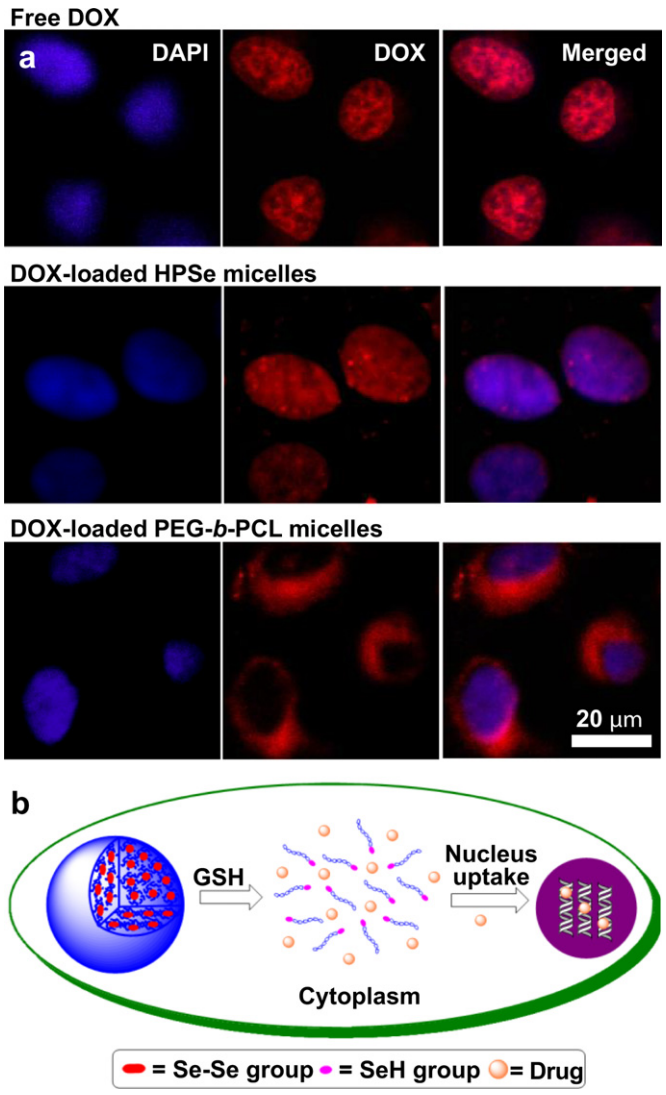

Fig. 8. (a) CLSM images of HeLa cells incubated with free DOX, DOX-loaded HPSe micelles or DOX-loaded PEG-*b*-PCL micelles for 3 h. The cell nuclei were stained by DAPI. (b) Illustration of HPSe micelles for intracellular drug release triggered by GSH.

intracellular GSH-mediated drug delivery of DOX-loaded HPSe micelles was then investigated in HeLa cells. It has been reported that free DOX quickly enters nuclei after cell uptake, whereas DOX transported by nonresponsive micelles accumulates in nuclei very slowly [52]. Free DOX and DOX-loaded nonresponsive micelles based on diblock copolymer of poly(ethylene glycol)-*b*-poly(ε-caprolactone) (PEG5k-*b*-PCL2k) were employed as positive and negative controls respectively. It was found that DOX fluorescence located at perinuclear region instead of the nucleus for PEG5k-*b*-PCL2k micelles, while fast accumulation of DOX in nuclei of HeLa cells was observed for both free DOX and DOX-loaded HPSe micelles (Fig. 8a). These results suggest that intracellular GSH induces the destabilization of HPSe micelles and triggers rapid release of the loaded drugs (Fig. 8b). Here HPSe plays the dual roles of highly efficient anticancer agent and smart drug carrier, which provides a new approach for combining therapy.

4. Conclusion

A hyperbranched polydiselenide with good solubility and stability has been successfully designed and synthesized. It consists of alternative hydrophobic diselenide and hydrophilic phosphate groups in the backbone framework. The HPSe exhibits a very potent anticancer effect for all sorts of cancer cells available here. The IC_{50} dose of HPSe in all of the tested cancer cell lines is within the concentration range between 1 and 2.5 μg mL^{-1} with the incubation time of 72 h. The cancer cell death induced by HPSe is attributed to the caspase-3 dependant apoptosis. It is demonstrated that the potent anticancer activities of HPSe come from the diselenide groups in the dendritic backbone. On the other hand, the amphiphilic HPSe can self-assembly into nanomicelles with an average diameter of 50 nm, and then spontaneously enter into tumor cells by EPR effect. So HPSe is a highly efficient, broad spectrum and self-delivery anticancer agent. In addition, HPSe micelles can be used as a drug carrier to encapsulate other hydrophobic anticancer drugs for combining therapy.

Acknowledgments

This work was supported by the National Basic Research Program (No. 2009CB930400, 2012CB821500), the National Natural Science Foundation of China (No. 91127047, 21174086, 21074069) and the China Postdoctoral Science Foundation (No. 2012M510834).

Appendix A. Supplementary data

The supplementary data associated with this article can be found, in the online version, at http://dx.doi.org/10.1016/j.biomaterials.2012.07.003.

References

[1] Duncan R. The dawning era of polymer therapeutics. Nat Rev Drug Discov 2003;2:347–60.
[2] Langer R, Tirrell DA. Designing materials for biology and medicine. Nature 2004;428:487–92.
[3] Lee CC, MacKay JA, Fréchet JMJ, Szoka FC. Designing dendrimers for biological applications. Nat Biotechnol 2005;23:1517–26.
[4] Gros L, Ringsdorf H, Schupp H. Polymeric antitumor agents on a molecular and on a cellular level? Angew Chem Int Ed 1981;20:305–25.
[5] Duncan R. Polymer conjugates as anticancer nanomedicines. Nat Rev Cancer 2006;6:688–701.
[6] Harris JM, Chess RB. Effect of pegylation on pharmaceuticals. Nat Rev Drug Discov 2003;2:214–21.
[7] Veronese FM, Harris JM. Introduction and overview of peptide and protein pegylation. Adv Drug Deliv Rev 2002;54:453–6.
[8] Masayuki Y, Mizue M, Noriko Y, Teruo O, Yasuhisa S, Kazunori K, et al. Polymer micelles as novel drug carrier: adriamycin-conjugated poly(ethylene glycol)-poly(aspartic acid) block copolymer. J Control Release 1990;11:269–78.
[9] Herold DA, Keil K, Bruns DE. Oxidation of polyethylene glycols by alcohol dehydrogenase. Biochem Pharmacol 1989;38:73–6.
[10] Matsumura Y, Maeda H. A new concept for macromolecular therapeutics in cancer chemotherapy: mechanism of tumoritropic accumulation of proteins and the antitumor agent smancs. Cancer Res 1986;46:6387–92.
[11] Ip C, Hayes C, Budnick RM, Ganther HE. Chemical form of selenium, critical metabolites, and cancer prevention. Cancer Res 1991;51:595–600.
[12] Rayman MP. The importance of selenium to human health. Lancet 2000;356:233–41.
[13] Clark LC, Alberts DS. Selenium and cancer: risk or protection? J Natl Cancer Inst 1995;87:473–5.
[14] Lu J, Jiang C, Kaeck M, Ganther H, Vadhanavikit S, Ip C, et al. Dissociation of the genotoxic and growth inhibitory effects of selenium. Biochem Pharmacol 1995;50:213–9.
[15] Thompson HJ. Selenium as an anticarcinogen. J Agric Food Chem 1984;32:422–5.
[16] Sanmartín C, Plano D, Domínguez E, Font M, Calvo A, Prior C, et al. Synthesis and pharmacological screening of several aroyl and heteroaroyl selenylacetic acid derivatives as cytotoxic and antiproliferative agents. Molecules 2009;14:3313–38.
[17] Sharma AK, Sharma A, Desai D, Madhunapantula SV, Huh SJ, Robertson GP, et al. Synthesis and anticancer activity comparison of phenylalkyl isoselenocyanates with corresponding naturally occurring and synthetic isothiocyanates. J Med Chem 2008;51:7820–6.
[18] Lin T, Ding Z, Li N, Xu J, Luo G, Liu J, et al. Seleno-cyclodextrin sensitises human breast cancer cells to TRAIL-induced apoptosis through DR5 induction and NF-jB suppression. Eur J Cancer 2011;47:1890–907.
[19] Combs Jr GF, Gray WP. Chemopreventive agents: selenium. Pharmacol Ther 1998;79:179–92.
[20] Parnham MJ, Graf E. Pharmacology of synthetic organic selenium compounds. Prog Drug Res 1991;36:9–47.
[21] Mugesh G, du Mont W-W, Sies H. Chemistry of biologically important synthetic organoselenium compounds. Chem Rev 2001;101:2125–80.
[22] Davis FF. The origin of pegnology. Adv Drug Deliv Rev 2002;54:457–8.
[23] Ferber D. Gene therapy: safer and virus-free? Science 2001;294:1638–42.
[24] Satchi-Fainaro R, Duncan R, Barnes CM. Polymer therapeutics for cancer: current status and future challenges. Adv Polym Sci 2006;193:1–65.
[25] Dhal PK, Holmes-Farley SR, Huval CC, Jozefiak TH. Polymers as drugs. Adv Polym Sci 2006;192:9–58.
[26] Twaites B, de las Heras Alarcón C, Alexander C. Synthetic polymers as drugs and therapeutics. J Mater Chem 2005;15:441–55.
[27] Seymour L. Review: synthetic polymers with intrinsic anticancer activity. J Bioact Compat Pol 1991;6:178–216.
[28] Ferrari M. Cancer nanotechnology: opportunities and challenges. Nat Rev Cancer 2005;5:161–71.
[29] Torchilin VP. Recent advances with liposomes as pharmaceutical carriers. Nat Rev Drug Discov 2005;4:145–60.
[30] Davis ME, Chen Z, Shin DM. Nanoparticle therapeutics: an emerging treatment modality for cancer. Nat Rev Drug Discov 2008;7:771–82.
[31] Nishiyama N, Kataoka K. Current state, achievements, and future prospects of polymeric micelles as nanocarriers for drug and gene delivery. Pharmacol Ther 2006;112:630–48.
[32] Mammen M, Choi S-K, Whitesides GM. Polyvalent interactions in biological systems: implications for design and use of multivalent ligands and inhibitors. Angew Chem Int Ed 1998;37:2754–94.
[33] Liu JY, Huang W, Pang Y, Huang P, Zhu XY, Zhou YF, et al. Molecular self-assembly of a homopolymer: an alternative to fabricate drug-delivery platforms for cancer therapy. Angew Chem Int Ed 2011;50:9162–6.
[34] Liu JY, Huang W, Zhou YF, Yan DY. Synthesis of hyperbranched polyphosphates by self-condensing ring-opening polymerization of HEEP without catalyst. Macromolecules 2009;42:4394–9.
[35] Chen M, Ona VO, Li M, Ferrante RJ, Fink KB, Zhu S, et al. Minocycline inhibits caspase-1 and caspase-3 expression and delays mortality in a transgenic mouse model of Huntington disease. Nat Med 2000;6:797–801.
[36] Liu JY, Pang Y, Huang W, Huang XH, Meng LL, Zhu XY, et al. Bioreducible micelles self-assembled from amphiphilic hyperbranched multiarm copolymer for glutathione-mediated intracellular drug delivery. Biomacromolecules 2011;12:1567–77.
[37] Günther WHH, Salzman MN. Methods in selenium chemistry IV. Synthetic approaches to polydiselenides. Ann N Y Acad Sci 1972;192:25–43.
[38] Ma N, Li Y, Xu H, Wang Z, Zhang X. Dual redox responsive assemblies formed from diselenide block copolymers. J Am Chem Soc 2010;132:442–3.
[39] Zhang X, Xu H, Dong Z, Wang Y, Liu J, Shen J. Highly efficient dendrimer-based mimic of glutathione peroxidase. J Am Chem Soc 2004;126:10556–7.
[40] Voit BI, Lederer A. Hyperbranched and highly branched polymer architectures-synthetic strategies and major characterization aspects. Chem Rev 2009;109:5924–73.
[41] Carlmark A, Hawker C, Hult A, Malkoch M. New methodologies in the construction of dendritic materials. Chem Soc Rev 2009;38:352–62.
[42] Calderón M, Quadir MA, Sharma SK, Haag R. Dendritic polyglycerols for biomedical applications. Adv Mater 2010;22:190–218.
[43] Wilms D, Stiriba SE, Frey H. Hyperbranched polyglycerols: from the controlled synthesis of biocompatible polyether polyols to multipurpose applications. Acc Chem Res 2010;43:129–41.
[44] Du W, Xu Z, Nyström AM, Zhang K, Leonard JR, Wooley KL. ^{19}F- and fluorescently labeled micelles as nanoscopic assemblies for chemotherapeutic delivery. Bioconjug Chem 2008;19:2492–8.
[45] Wang YC, Yuan YY, Du JZ, Yang XZ, Wang J. Recent progress in polyphosphoesters: from controlled synthesis to biomedical applications. Macromol Biosci 2009;9:1154–64.
[46] Zhao Z, Wang J, Mao HQ, Leong KW. Polyphosphoesters in drug and gene delivery. Adv Drug Deliv Rev 2003;55:483–99.
[47] Liu JY, Pang Y, Huang W, Zhai X, Zhu XY, Zhou YF, et al. Controlled topological structure of copolyphosphates by adjusting pendant groups of cyclic phosphate monomers. Macromolecules 2010;43:8416–23.
[48] Ghosh J. Rapid induction of apoptosis in prostate cancer cells by selenium: reversal by metabolites of arachidonate 5-lipoxygenase. Biochem Biophys Res Commun 2004;315:624–35.
[49] Zhou J, Chen R. Synthesis and crystal structure of 2-phosphonoalkyl-1, 2-benzisoselenazol-3(2H)-ones and their antitumor activities. Heteroat Chem 1999;10:247–54.
[50] Krepela E. Cysteine proteinases in tumor cell growth and apoptosis. Neoplasma 2001;48:332–49.
[51] Kabanov AV. Polymer genomics: an insight into pharmacology and toxicology of nanomedicines. Adv Drug Deliv Rev 2006;58:1597–621.
[52] Liu JY, Huang W, Pang Y, Zhu XY, Zhou YF, Yan DY. Self-assembled micelles from an amphiphilic hyperbranched copolymer with polyphosphate arms for drug delivery. Langmuir 2010;26:10585–92.